

# How Transformer DC Winding Resistance Testing Can Cause Generator Relays to Operate

Ritwik Chowdhury, Mircea Rusicior, Jakov Vico, and Jason Young  
*Schweitzer Engineering Laboratories, Inc.*

© 2016 IEEE. Personal use of this material is permitted. Permission from IEEE must be obtained for all other uses, in any current or future media, including reprinting/republishing this material for advertising or promotional purposes, creating new collective works, for resale or redistribution to servers or lists, or reuse of any copyrighted component of this work in other works.

This paper was presented at the 69th Annual Conference for Protective Relay Engineers and can be accessed at: <https://doi.org/10.1109/CPRE.2016.7914888>.

For the complete history of this paper, refer to the next page.

Presented at the  
43rd Annual Western Protective Relay Conference  
Spokane, Washington  
October 18–20, 2016

Originally presented at the  
69th Annual Conference for Protective Relay Engineers, April 2016

# How Transformer DC Winding Resistance Testing Can Cause Generator Relays to Operate

Ritwik Chowdhury, Mircea Rusicior, Jakov Vico, and Jason Young, *Schweitzer Engineering Laboratories, Inc.*

**Abstract**—DC winding resistance testing of a power transformer increases the residual flux of the transformer. If it is not demagnetized following the testing, the transformer retains a high level of residual flux. Therefore, when the transformer is returned to service, the voltage required to drive the transformer into saturation is decreased. When a generator step-up transformer is returned to service following this testing, significant magnetizing current is drawn as the field voltage is increased. This large magnetizing current has the potential to cause sensitive generator protection elements to incorrectly operate. In this paper, a real-world event and simulations are used to study the impact of dc winding resistance testing on the magnetizing current of a transformer. Solutions are provided to mitigate possible unintended operations.

## I. INTRODUCTION

Large power transformers are very valuable and expensive assets that are key to the operation of the electric power system. This includes generator step-up (GSU) transformers that connect generators to the transmission system.

Many of these transformers are approaching or have already exceeded their expected lifespan. According to a U.S. Department of Energy report in 2012, 70 percent of large power transformers on the power system in the United States were over 25 years old, with the overall average transformer age being 40 years [1].

With aging infrastructure, the routine maintenance and testing of large power transformers has become increasingly necessary to ensure that the equipment remains in good working condition. GSUs are especially important because a failure results in a loss of generation.

One commonly used transformer test is direct current (dc) winding resistance testing. Unless the transformer is intentionally demagnetized following this test, significant residual flux remains in the transformer. When the unit is returned to service, the currents and voltages seen during energization can differ from typical values. These changes in current and voltage have the potential to modify the response of generator and transformer protection relays when the unit is energized for the first time following the testing. This paper focuses specifically on the resulting impact on generator relays. Refer to [2] for details on how ultra-saturation can affect transformer relay operation.

The paper explores a real-world case in which a GSU transformer dc winding resistance test adversely affected the currents and voltages seen by the generator protection relay when the unit was returned to service, resulting in an undesired operation of the protection system as the field was ramped. A detailed analysis of what happened and why it occurred is provided, as well as an overview of some potential improvements that can be made to enhance scheme security.

## II. DC WINDING RESISTANCE TESTING

### A. Testing Procedure

DC winding resistance testing is performed during transformer commissioning, after the occurrence of internal faults, and during periodic maintenance as recommended by the manufacturer [3]. Winding resistance tests are performed to assess the integrity of a transformer's windings, tap changer, and internal connections.

There are three primary methods for conducting winding resistance tests: the voltmeter-ammeter method, the bridge method, and the micro-ohmmeter method. The voltmeter-ammeter method is the most common, and it typically consists of connecting a dc source across each separate phase for wye-connected windings, or between each pair of phases for delta-connected windings, with all other terminals open. The measured current and voltage are used to calculate the winding resistance, which is then compared amongst the three windings and with original data measured at the factory. Agreement within 5 percent is considered satisfactory [3]. Fig. 1 shows a typical test setup.

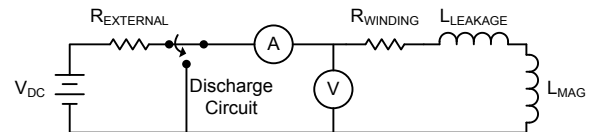


Fig. 1. Typical voltmeter-ammeter dc winding resistance test setup

There are a number of considerations that must be taken into account when performing dc winding resistance testing, such as connection configuration, current and voltage test levels, temperature compensation, and safety. A detailed discussion of these points is beyond the scope of this paper. Refer to [3], [4], and [5] for more information on dc winding resistance testing procedures.

### B. Transformer Magnetics

In order to understand the protective relay response, it is necessary to know the effect of this test on the magnetic circuit of the transformer. Based on Fig. 1, an equation can be written to express the voltage measured by the voltmeter as a function of the current in the circuit and the  $R$  and  $L$  winding values, as shown in (1).

$$V(t) = R_w \cdot I(t) + L_w \cdot \frac{dI(t)}{dt} \quad (1)$$

where:

$V$  is the voltage measured by the voltmeter.

$I$  is the current measured by the ammeter.

$R_w$  is the winding resistance.

$L_w$  is the winding inductance (leakage and magnetizing).

In (1),  $R_w$  is the term that must be measured. To do so accurately, the effect of the derivative term must be minimized. This is accomplished by keeping the test current constant over time, avoiding low flux densities, and trying to reach saturation of the core.

However, when the dc source is applied, it acts as a step change. This results in a transient period where the voltage across the winding inductance ( $L_w$ ) decays exponentially from the initial value to zero. The magnetizing current rises exponentially to a steady-state value, limited by the resistance in the circuit. This behavior is illustrated in Fig. 2.

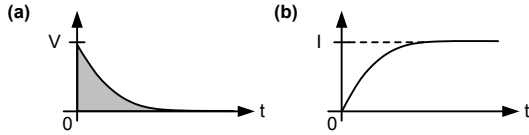


Fig. 2. Magnetization voltage (a) and current (b) transient response to an applied dc test voltage

By waiting for the current to reach the steady state, the criteria for accurately measuring the winding resistance are met. During this transient period, the transformer core is driven into saturation as the flux is increased.

The flux is given by the integral of magnetizing voltage over time, as defined in (2). This corresponds to the area under the curve of voltage across the magnetizing inductance. The shaded region in Fig. 2a illustrates this relationship as it relates to the dc winding resistance test.

$$\Phi = \frac{1}{N} \int v(t) dt \quad (2)$$

where:

$\Phi$  is the flux.

$N$  is the number of turns on the winding under test.

$v(t)$  is the voltage across the magnetizing branch.

In the case of dc winding resistance testing, the voltage applied is shown by (3). Plugging this into (2) gives the value of residual flux in the transformer.

$$v(t) = V \cdot e^{\left(\frac{-t}{\frac{L_w}{R_w}}\right)} \quad (3)$$

Fig. 3 shows a typical hysteresis curve for a magnetic material. The loops represent the relationship between the magnetomotive force (mmf) produced by the current ( $\mathcal{F} = N \cdot I$ ) and the amount of flux produced in the core. The mmf and flux follow this characteristic each cycle for an applied alternating current (ac) voltage. As the magnitude of the applied voltage is increased, the size of the loop increases accordingly. Fig. 3 shows two cases; the applied voltage and current for Loop 2 are greater than those for Loop 1.

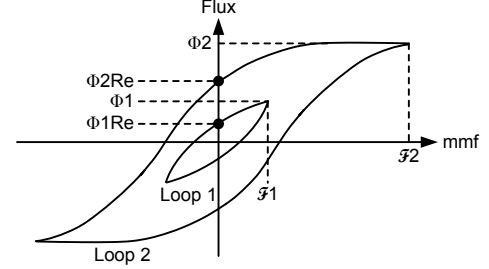


Fig. 3. Typical transformer core hysteresis curve

If the ac voltage is increased enough, the core enters saturation. The effect of saturation is seen at the extremes of Loop 2, such as point  $(\mathcal{F}_2, \Phi_2)$ , in Fig. 3. In Loop 1, an increase in magnetic flux results in a proportional increase in mmf. However, at the extremes of Loop 2, when the transformer reaches saturation, a small increase in flux results in a large increase in mmf because the transformer core has reached its maximum flux density. Because the excitation current is proportional to mmf, this also implies that a small increase in flux causes a large increase in excitation current.

The magnetizing inductance ( $L_{MAG}$ ) is proportional to the slope of the hysteresis curve. Reaching saturation therefore lowers the inductance of the system under test.

In the case of the dc winding resistance test, a dc voltage is applied instead of an ac voltage. Therefore, the flux in the core does not circulate around a loop as shown in Fig. 3, but rather increases in one direction proportional to the area under the voltage curve in Fig. 2. Because the flux is additive over time, the core is driven to saturation, which is the ideal state for taking the winding resistance measurements.

Upon test completion, the voltage source is removed and the winding is switched to the discharge circuit per Fig. 1. This causes a decaying negative voltage to appear across the winding, driving the current to zero within a time given by the time constant  $L/R$  of the winding. The negative voltage causes a reduction in flux that can be traced to the point where the top line of the excitation curve intercepts the y-axis. The point  $\Phi_{2Re}$  represents the residual flux after the transformer has been driven to saturation.

Note that this residual flux can be removed with additional procedures, but this step is not always completed [6]. Therefore, the transformer is often returned to service with residual flux in the core.

### C. Re-Energizing a GSU Transformer With Residual Flux

This subsection focuses specifically on the re-energization of unit-connected GSU transformers from the generator,

which pertains directly to the case study in Section IV. Implications for other configurations are provided as well.

Typically, when a unit-connected generator is brought online, the generator is brought up to speed and the field is applied with the GSU transformer connected. When the field is applied, the voltage is increased to nominal over a period of a few seconds. The exact amount of time depends on the system. Regardless of the ramp rate, the voltage applied to the transformer is built up over time rather than instantly applied, as is the typical case in other parts of the power system. The result is that there is often very little magnetizing current drawn by the transformer.

When the GSU transformer has zero residual flux in the core prior to energization, the resulting hysteresis loop (Fig. 3) is centered at the origin and grows with the applied voltage. Through the entire voltage ramp, the flux in the core aligns with the linear portion of the transformer excitation curve, resulting in a small excitation current, as shown in Fig. 4.

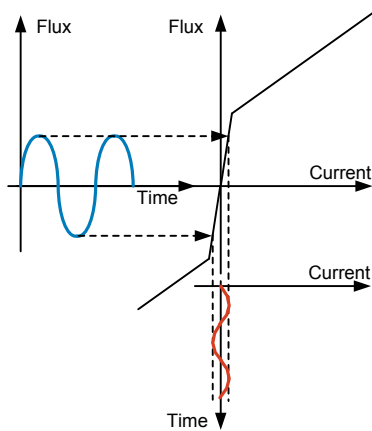


Fig. 4. Excitation current and flux relationship with no residual flux

When the GSU transformer is made up of three single-phase transformers, the magnetic flux within the three cores does not need to balance, and each core can saturate independently. Assuming that each of the three cores has undergone the same dc winding resistance test, it can be expected that all three cores will have a similar amount of residual flux. Therefore, it is also expected that the excitation current seen on all three phases will resemble the characteristic shown in Fig. 5. However, because the voltages applied to the three single-phase transformers are separated by 120 electrical degrees, it is expected that the spikes in excitation current between the three phases will also be offset by 120 degrees.

In contrast, when the transformer has residual flux in the core prior to energization, the change in flux developed by the applied voltage begins from the residual flux point rather than the origin. If the first half cycle of the applied voltage is of the same polarity as the residual flux, the voltage magnitude required to drive the core into saturation will be less than that for a transformer with no residual flux and will be relative to the amount of residual flux. When the transformer is driven into saturation, high amounts of excitation current are drawn, as shown in Fig. 5.

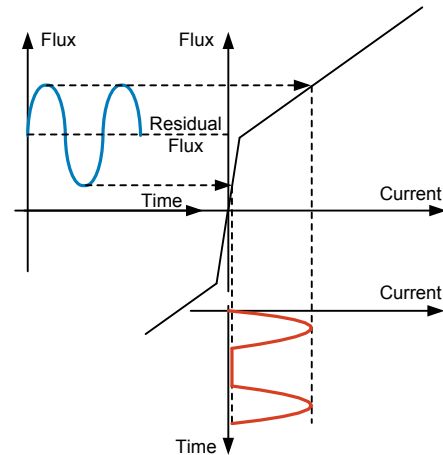


Fig. 5. Excitation current and flux relationship with significant positive residual flux

It is important to note that most GSU transformers are connected in delta on the generator side, with the polarity of the A-phase connected to the nonpolarity of the C-phase (DAC connection). As such, the voltage across each of the three single-phase transformers is phase-to-phase (i.e., Core A = VAB, Core B = VBC, and Core C = VCA).

The current transformers (CTs) do not measure the current inside the delta winding. Therefore, the saturation of one core causes current to flow into the winding from the phase connected to the winding polarity and out of the phase connected to the winding nonpolarity. Fig. 6 shows the currents seen by the phase CTs for each of the saturating cores (shaded).

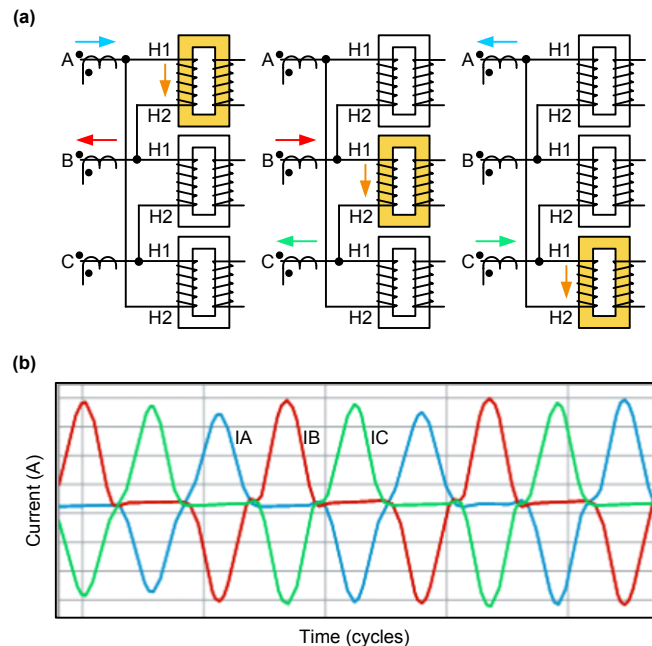


Fig. 6. Inrush current for three DAC-connected single-phase transformers, including saturated transformer cores (a) and example inrush current waveforms (b)

For instance, if the A-phase core saturates, a high amount of current flows into the winding on the A-phase and out of the winding on the B-phase. Because the CT polarity is away

from the transformer, the protective relay sees positive A-phase current and negative B-phase current. Because the other two cores are not saturated at the same time, only minimal excitation current flows through those windings.

In many applications, the GSU transformer is a single three-phase transformer with a three-legged core construction. In such cases, the fluxes in the three legs of the core must balance each other. The flux in the core of the transformer behaves in an analogous manner to current in an electric circuit: flux flowing into a node must equal the flux flowing out of the node. Fig. 7 illustrates this principle by showing different states that can be seen in every cycle during the energization of a three-legged core transformer. Note that state (c) is not valid because it violates this principle.

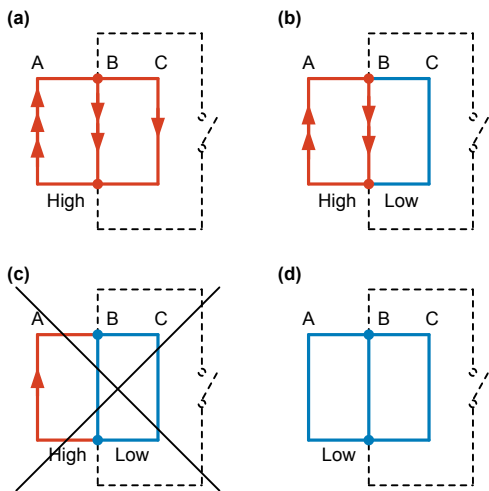


Fig. 7. Flux in a three-legged, three-phase transformer during inrush

In Fig. 7, each solid vertical line represents a specific leg of the transformer and its corresponding winding. The red lines (with arrowheads) indicate varying levels of saturation and flux, while the blue lines (without arrowheads) indicate legs that are not saturated and thus have a lower amount of flux. Note that the amount of magnetizing current in each phase is proportional to the flux and is represented by the number of arrows. As explained in [2], the typical sequence of flux shown in Fig. 7 is to progress from state (a) to (b) to (d).

The transformer winding that underwent dc resistance testing last will have the highest amount of magnetic saturation. The other two legs will also have a considerable amount of saturation, but in the reverse direction. The sum of the residual fluxes in these two cores corresponds to the residual flux in the core tested last, though reverse in polarity. This results in high unipolar currents on one winding along with lower currents of opposite polarity on the other two. Fig. 8 shows an example of the inrush current to a GSU transformer as the field was ramped to nominal voltage following dc winding resistance testing.

The three-phase, three-legged transformer is really a special case of three single-phase transformers, with the additional constraint that the sum of the fluxes of the three legs is zero.

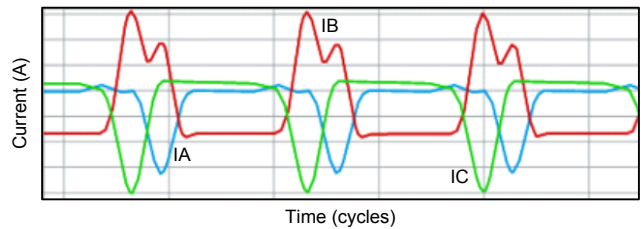


Fig. 8. Inrush currents in a DAC-connected, three-legged core transformer with residual flux during field ramping

In other applications, the GSU transformer is not connected to the generator before the field is applied, but rather the generator main breaker is closed following the application of the field. The result of residual flux in these applications is that there is a potential for the inrush current to be higher than normal as the transformer is driven further into saturation. As discussed previously, the degree of saturation depends on the magnitude and polarity of the residual flux and the initial half cycle of voltage.

### III. EFFECT ON GENERATOR PROTECTION ELEMENTS

Most generator protection elements are designed to maintain security during inrush current, including inrush resulting from the residual flux left in the transformer following dc winding resistance testing. This section provides an overview of some specific generator protection elements and how they respond during inrush conditions.

#### A. Third-Harmonic Voltage Elements for 100 Percent Stator Ground Protection

The fundamental neutral voltage has traditionally been used to detect ground faults in high-resistance-grounded generators. The fundamental neutral voltage rises for ground faults, reaching its maximum magnitude for faults at the generator terminals and decreasing as the fault location moves closer to the neutral point. However, the neutral overvoltage element (59N or 64G1) does not protect a region of about 5 percent of the winding length, starting from the neutral point. Third-harmonic voltages are generated by most machines and are commonly used to detect such faults. A fundamental neutral overvoltage scheme, combined with a third-harmonic-based protection scheme, provides coverage for 100 percent of the stator winding.

During normal operation, the third-harmonic voltage at the neutral is not in phase with the third-harmonic voltage at the generator terminal. Both neutral and terminal third-harmonic voltages typically increase in magnitude for higher power outputs, as shown in Fig. 9a. Ground faults near the neutral point cause the neutral third-harmonic voltage  $V_{3N}$  to decrease in magnitude and the terminal third-harmonic voltage  $V_{3P}$  to increase in magnitude, as shown in Fig. 9b. Ground faults close to the generator terminals increase the magnitude of the neutral third-harmonic voltage and decrease the magnitude of the terminal third-harmonic voltage, as shown in Fig. 9c.

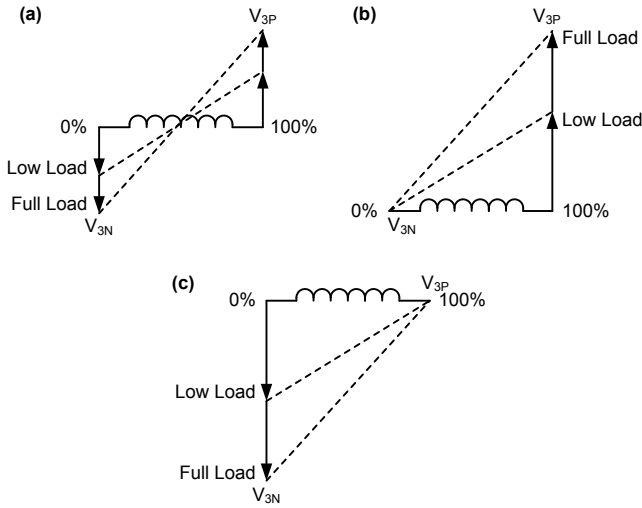


Fig. 9. Third-harmonic voltage in a typical generator for normal operation (a), a ground fault at the machine neutral (b), and a ground fault at the machine terminals (c)

Faults near the neutral of the generator can be detected with a third-harmonic neutral undervoltage element (27TN or 64G2), a third-harmonic terminal overvoltage element (59T or 64G2), or a third-harmonic differential element (59THD or 64G2). The differential scheme involves a comparison of the third-harmonic voltages measured at the terminals and at the neutral of the generator.

All third-harmonic schemes are intended to complement and overlap the coverage provided by the 59N element. Fig. 10 illustrates the protection coverage provided by the combination of the 59N neutral overvoltage element and the 59THD third-harmonic differential element. Both of these elements cannot identify faults within specific regions of the winding. These regions are called dead bands. Because the dead band of the 59N element is near the neutral, and that of the 59THD element is near the middle of the winding, the two elements can be used together to cover the entire winding.

A typical operate equation for the third-harmonic voltage differential element 59THD is provided in (4).

$$|59THD_{RAT} \cdot V_{3P} - V_{3N}| > 59THD_{PU} \quad (4)$$

where:

$V_{3P}$  is the third-harmonic voltage magnitude at the generator terminals in per unit (pu).

$V_{3N}$  is the third-harmonic voltage magnitude at the neutral in pu.

$59THD_{RAT}$  is a relay setting in pu, selected to balance the differential element over the generator load range.

$59THD_{PU}$  is the third-harmonic differential pickup setting in pu, which must be above the highest differential voltage.

Because each machine is different, the third-harmonic element settings must be calculated using data from field measurements during commissioning. The terminal and neutral third-harmonic voltage magnitudes should be recorded as the generator is run through as many operating conditions as possible. This includes ramping the generator to full load and varying the power factor.

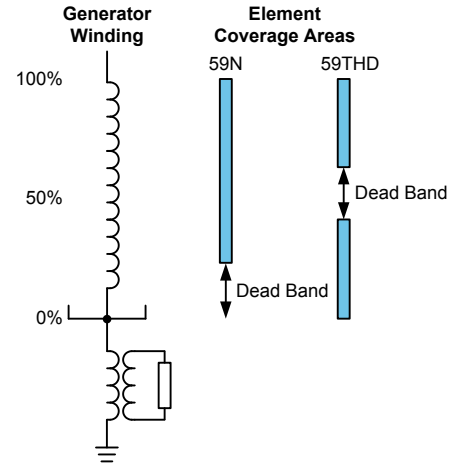


Fig. 10. Stator winding coverage of the 59N and 59THD elements

When the distribution of the third-harmonic changes little with load, the procedure described above can result in a sensitive setting for this element. When the GSU transformer is energized following dc winding resistance testing, the inrush current can result in small distortions of the voltage, altering the third-harmonic voltages measured by the relay. This point will be discussed in greater detail during the analysis of the case study.

### B. Inadvertent Energization

The *IEEE Tutorial on the Protection of Synchronous Generators* recommends using dedicated protection schemes for detecting an inadvertent energization condition [7]. These dedicated schemes include the use of a directional overcurrent element, a distance relay, or a supervised overcurrent element. Supervisory options for the overcurrent elements include frequency, voltage, field breaker status, or a combination of these [7]. Fig. 11 shows typical logic for a voltage-supervised overcurrent element.

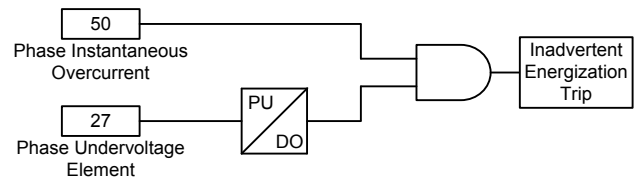


Fig. 11. Voltage-supervised overcurrent element inadvertent energization scheme [7]

According to IEEE, the overcurrent relay should be set for 50 percent of the minimum inadvertent energization current [7]. If the generator can be energized through the station service transformer, this current can be much lower than when energized inadvertently through the GSU transformer. As a result, the overcurrent pickup can be set very sensitively. Therefore, depending on the pickup setting of the undervoltage element and the dropout time delay, it is possible that this element could assert in response to the inrush currents seen when returning the unit to service following dc winding resistance testing. The rate at which the field is applied also affects the operation of this element.

A more secure option is to supervise the overcurrent element with multiple elements. Typical logic for this scheme is shown in Fig. 12.

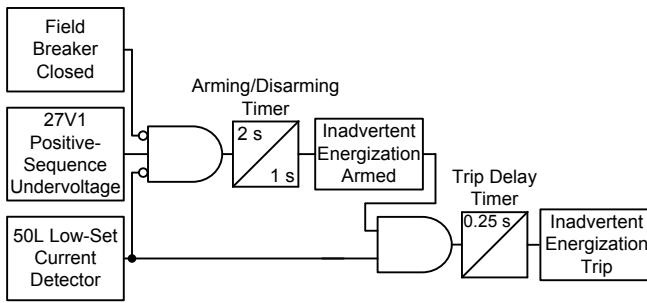


Fig. 12. Inadvertent energization scheme: overcurrent element supervised by multiple elements [7]

This scheme has the advantage that the disarming timer begins timing as soon as the field breaker is closed rather than waiting until the voltage exceeds the undervoltage element pickup threshold. Despite this added benefit, the overall scheme security depends on the voltage ramp rate, the pickup settings used, and the time delays selected for the logic.

### C. Phase Differential Elements

Generator phase differential elements are often set sensitively. This is considered acceptable, provided that the CTs and the connected burdens are matched. However, when the CTs are exposed to large inrush currents, the offset waveforms can cause CT saturation which, if not equivalent in both CTs, results in false differential current.

This is of particular concern in applications where the GSU transformer is energized by closing the generator breaker following bringing the generator to rated speed and voltage. The residual flux in the transformer caused by dc winding resistance testing can cause greater inrush current than normal, increasing the probability of CT saturation and false differential current. Security can be added to a phase differential scheme by using an adaptive element, as described in [8].

Note that the concern for this element is specific to three-phase transformers. Fig. 8 shows that the current seen in each phase is unipolar for a three-legged, three-phase transformer. As a result, the flux in the CT builds up in one direction, and can result in dc saturation. However, in applications where three single-phase transformers are used (Fig. 6b), the current in each phase CT has both positive and negative half-cycles that are similar in magnitude. Therefore, the flux does not build up in one direction. Because the inrush currents seen are relatively small (1 pu or less), CT saturation is unlikely.

## IV. CASE STUDY: GENERATOR THIRD-HARMONIC ELEMENT OPERATION

A 575 MVA steam generating unit was connected through three single-phase transformers to the grid. Before synchronizing to the grid, the generator was brought up to rated speed and the field was applied to bring it up to rated voltage in 5 seconds. Fig. 13 shows the one-line diagram of the generator.

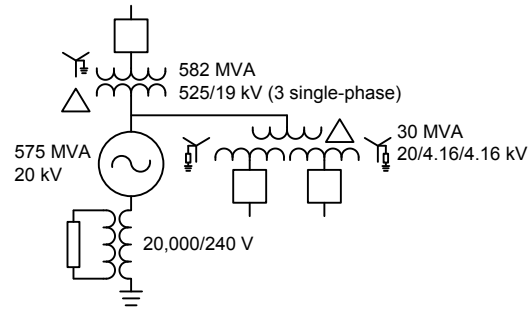


Fig. 13. Unit-connected generator one-line diagram

The generator relay issued a trip command that tripped the field breaker and turbine as the machine was being brought up to rated voltage. This section provides an analysis of this event and compares the results to data obtained from simulations.

### A. Third-Harmonic Differential Element

#### 1) Event Analysis

Fig. 14 shows the unfiltered event report data collected from the generator relay following the trip. Note that the rated current is 16.6 kA.

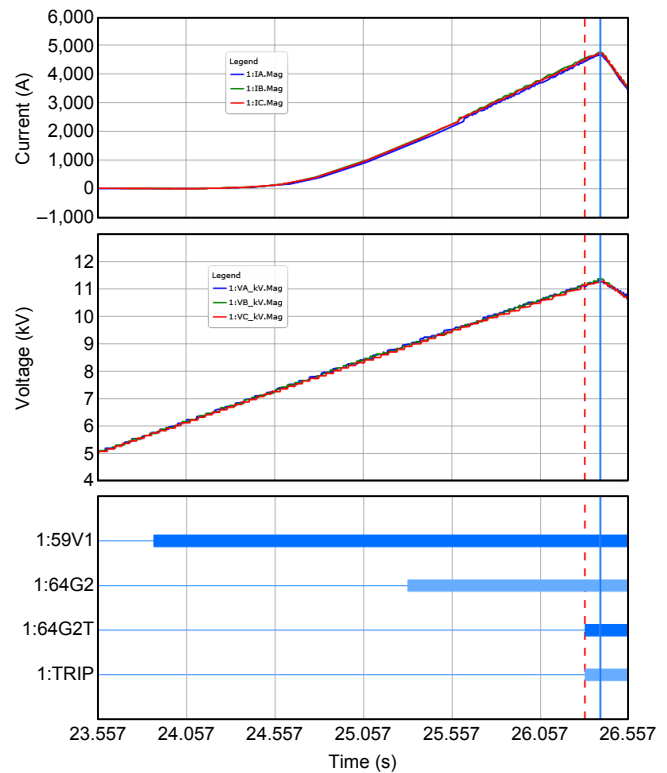


Fig. 14. Operation of the third-harmonic differential element during field ramp

The terminal phase voltages were ramping up to nominal when the relay issued the trip at 11 kV. The phase currents were initially negligible, but started increasing when the phase voltages exceeded 7 kV. When the voltage magnitude reached 11 kV, nearly 5 kA phase currents were being drawn from the machine. The main breaker on the grid side of the GSU was open. The auxiliary breakers on the low-voltage side of the auxiliary transformer were also open. As shown in Fig. 14, the

third-harmonic element (64G2T) tripped the breaker as the field was being ramped.

The third-harmonic element for a given machine typically follows a fairly well-bounded ratio profile, as discussed in Section III. In Fig. 15, the third-harmonic voltage data captured during a load run are plotted along with the third-harmonic element pickup setting. The pickup setting of the third-harmonic element provides upper and lower thresholds that are observed during normal operation of the generator. The element restraint region lies between these thresholds. At a given point in the event, the third-harmonic profile exceeded the upper tolerance of the element and the relay operated.

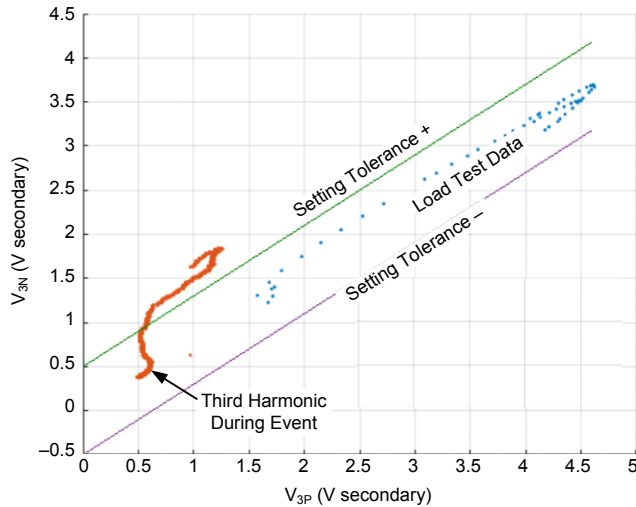


Fig. 15. Third-harmonic voltages measured by the relay during load and event

As shown in Fig. 16, the third-harmonic voltage profile as the field was applied deviated significantly from the standard third-harmonic profile data captured during a load run.

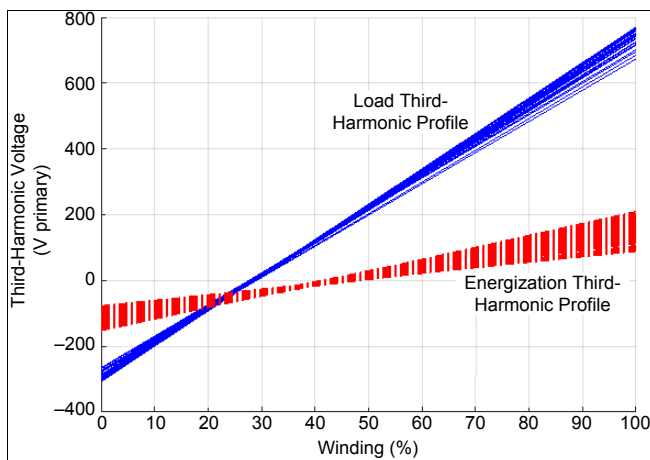


Fig. 16. Third-harmonic voltage profile during load and energization at different winding regions

The profile during this energization was not simply shifted with the same overall magnitude of third-harmonic voltage generated across the generator stator winding, as expected for a fault condition. Instead the third-harmonic voltage across the winding was significantly reduced in magnitude. This is not typical for a fault.

Despite the magnitude deviation, the neutral third-harmonic voltage is still expected to be approximately zero for a fault near the neutral of the stator winding. However, if there is a fault in another portion of the winding, fundamental voltage is measured across the neutral grounding resistor corresponding to the fault location. As shown in Fig. 17, however, there was no voltage imposed at the machine neutral as the terminal voltage was increased to nominal. This rules out the possibility of a ground fault within the generator, on the connected isophase bus, or in the delta windings of the GSU or station service transformers.

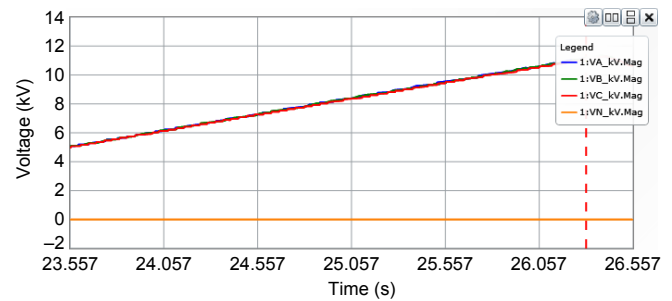


Fig. 17. Fundamental phase and neutral voltage magnitudes measured by the relay during the event

In order to analyze what occurred, a closer analysis of the voltage and current waveforms, as shown in Fig. 18, was required.

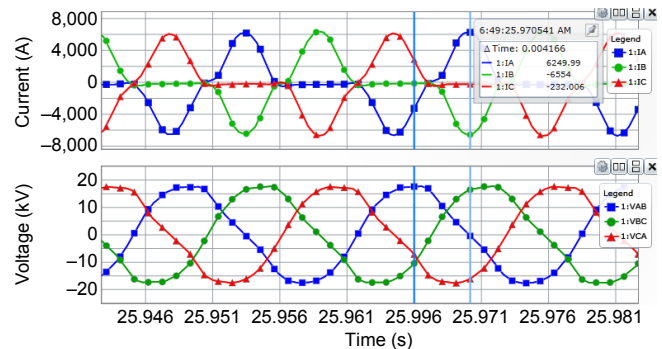


Fig. 18. Phase current and voltage phase relationship in event

The current waveforms are not typical of an inrush condition. Normally, when nominal voltage is directly applied to a transformer, the inrush currents vary between phases and exponentially decay, as shown in Fig. 19.

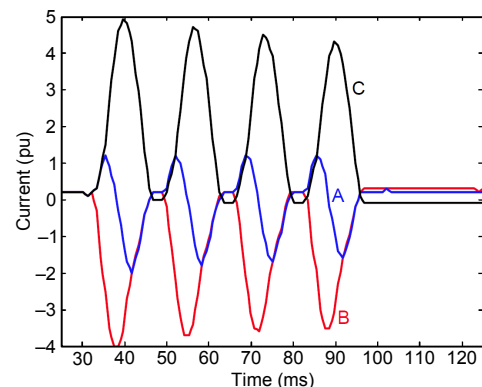


Fig. 19. Typical inrush currents for a three-legged core transformer energized with rated voltage

The variation in the phase currents is caused by varying levels of residual flux in the three phases and each of the phase breakers closing at different points on the voltage wave. In this case, the voltage was ramped from zero as the field was applied, minimizing this effect.

The gradual decay of the inrush current that is typically seen is caused by the magnetic hysteresis property of the core. The hysteresis causes the core to gradually come out of saturation, and the flux centers on the origin. When voltage is ramped to nominal, the currents do not decay immediately due to the voltage source increasing as the field excitation is ramping up. The voltage increase pushes the core deeper into saturation, resulting in a higher amount of inrush current. Once nominal voltage is reached, the effects of hysteresis cause a gradual decay of the inrush currents.

However, the waveform in Fig. 18 also differed significantly from that of a previous return to service of this unit. Fig. 20 shows the phase current and voltage magnitudes as the field was applied approximately one year earlier. In this case, the inrush current was less than 100 A, compared to almost 5 kA in the case of the trip.

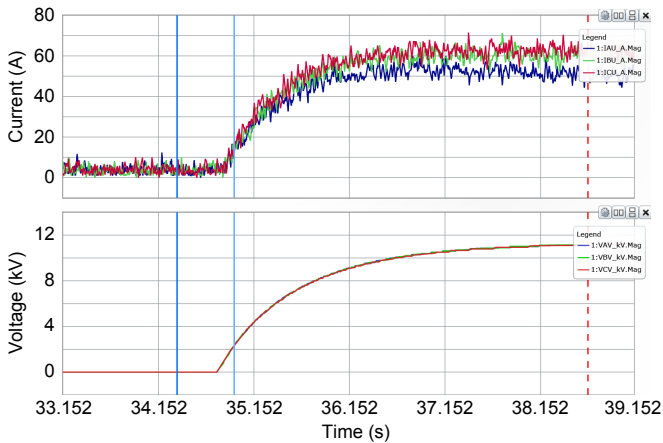


Fig. 20. Phase current and voltage magnitude from previous return to service

This drastic discrepancy prompted further investigation to understand the relationship between the third-harmonic element operation and the large inrush currents. From the raw event data at the time when the third-harmonic element asserted (Fig. 18), there was a 90-degree lag between the positive peak of each phase current and its corresponding phase-to-phase voltage peak. Because it was proven that there was no fault present on the system, this relationship matched the explanation in Section II, Subsection C. Given that all of the breakers were open, this high level of current could only be attributed to the low magnetizing inductance of the GSU transformer during saturation. The GSU transformer typically

draws less than 100 A of magnetizing current when the core is unsaturated, as shown in Fig. 20. This observation prompted questions as to the cause of such a heavy degree of saturation. It was later discovered that dc winding resistance testing had recently been performed on this transformer prior to its return to service.

A second third-harmonic differential trip occurred for this generator 25 minutes later when the field was being ramped again, as shown in Fig. 21. The voltage and current profiles observed in this case were similar to those shown in Fig. 14. However, the maximum inrush current magnitude was lower in this case—3.8 kA in the second event compared with 4.8 kA in the first event. The 64G2 element asserted when the terminal voltage reached 9.5 kV in contrast to 9.0 kV in the previous case. This was the result of a lower residual flux in the transformer following the first energization and trip. Further, at the solid blue vertical line in Fig. 21, the magnitude of inrush current starts to decrease prior to the relay trip (dotted red line). These differences are all indications that the GSU transformer was coming out of saturation because of the ac voltage applied to it.

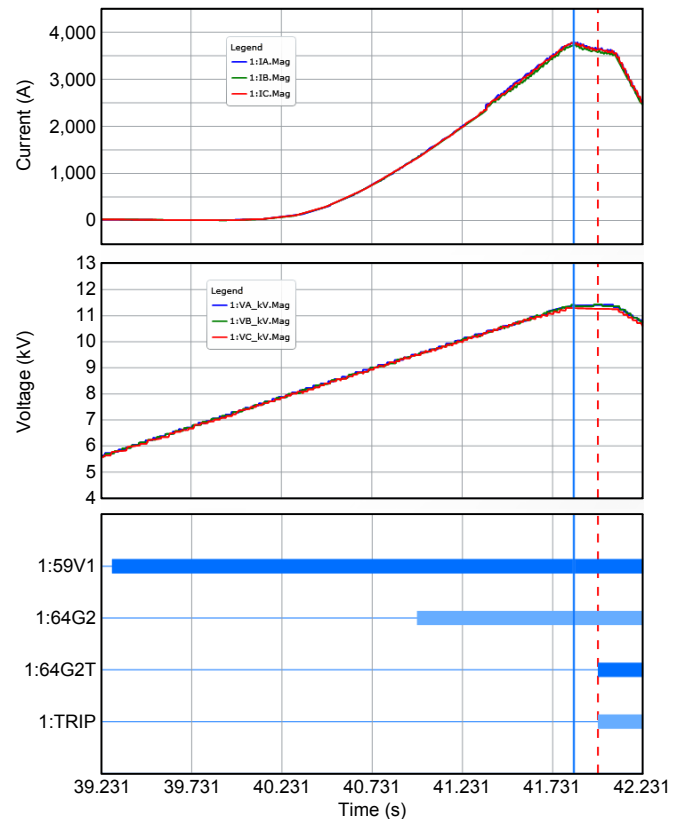


Fig. 21. Subsequent operation of the third-harmonic differential element with decaying inrush current

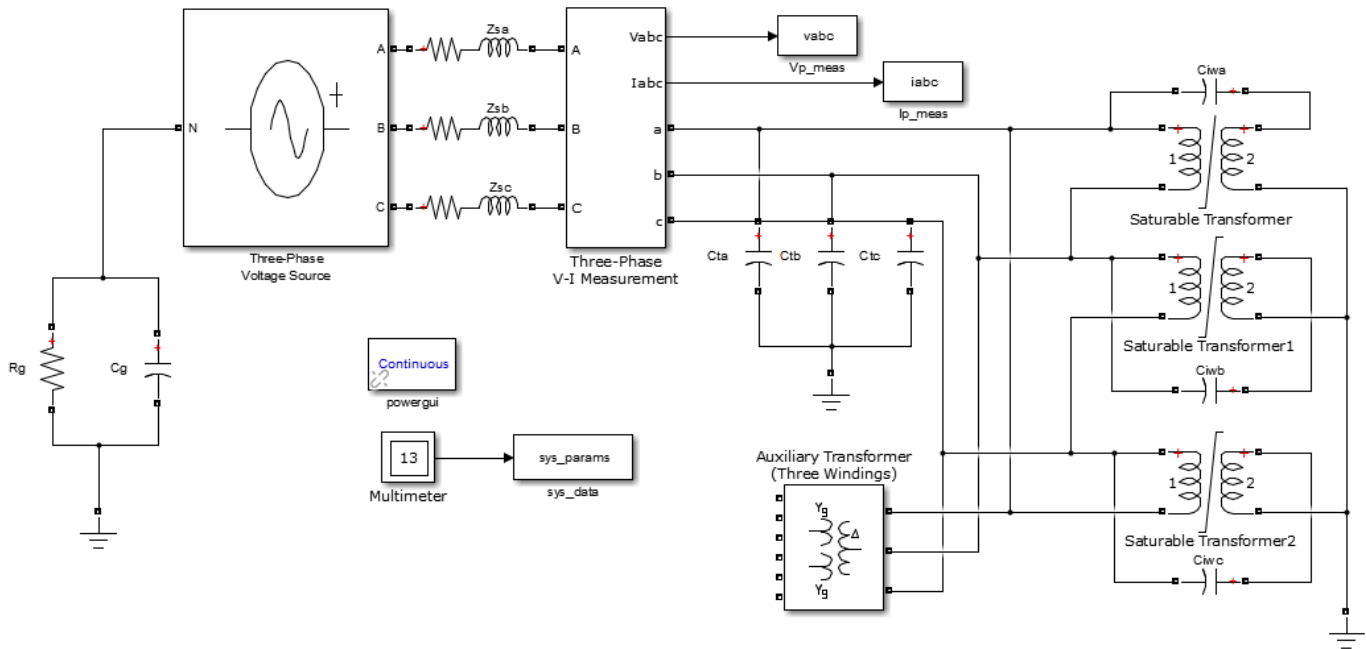


Fig. 22. System model as implemented in Simulink®

Because of core saturation, as explained in Section II, the transformer drew a high amount of magnetizing current. This sudden increase in current corresponded to a voltage distortion at the terminals of the machine, indicating harmonic content. The harmonic content in this voltage was not related to the generator's characteristic third-harmonic profile but was a byproduct of the core saturation of the GSU behaving as an external nonlinear circuit. The effect of this voltage distortion on the third-harmonic element is discussed in the following subsection. The current waveform was rich in second- and fourth-harmonic components, which is consistent with a transformer inrush condition.

## 2) Waveform Comparison Between Event and Simulation Data for Three Single-Phase Transformers

In order to study the phenomenon further, the system was modeled using Simulink, as shown in Fig. 22. An equivalent 60 Hz source model was used instead of a machine model in order to more clearly show the contribution of the transformer rather than the effect of the machine dynamics.

In the simulation, the source voltage was ramped from zero to nominal voltage in 5 seconds to match the actual machine. The three single-phase transformers were saturated evenly. As shown in Fig. 23, after the voltage was ramped up past 60 percent of its nominal voltage, the current began increasing dramatically, reaching a maximum value of approximately 5 kA at nominal voltage. This is consistent with the events shown in Fig. 14 and Fig. 21. After reaching nominal voltage, the inrush current started to decay immediately in both the

event and the simulation. After a few seconds, the inrush condition had dissipated and fewer than 100 A of magnetization current were drawn by the transformer in the model. This result matches the steady-state magnetization current measured in Fig. 20 from the previous return to service event capture.

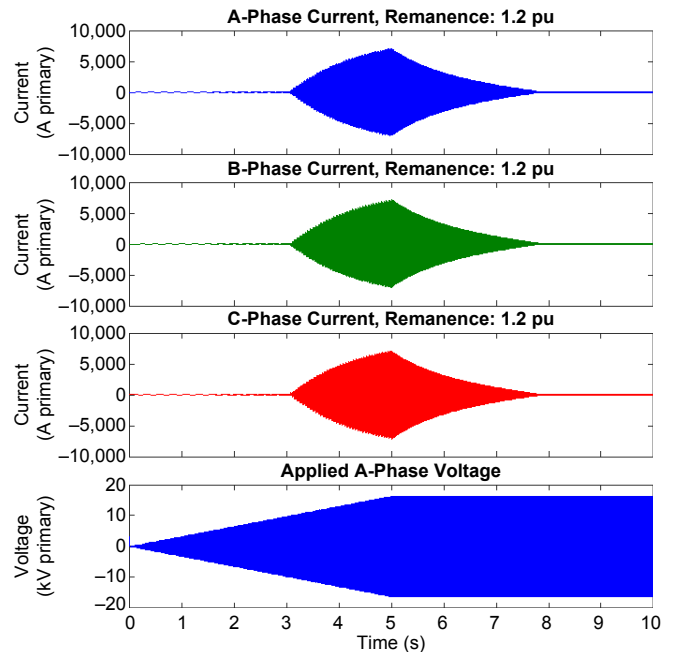


Fig. 23. Simulated current and voltage waveforms during inrush

Comparing the inrush waveform between the event and the simulation revealed some distinct similarities. The positive phase current peaks lag their associated phase-to-phase voltage peaks by 90 degrees, as shown in Fig. 18 (event) and Fig. 24 (simulation). The distortions in the voltages also coincide with the sudden increase and decrease of the currents.

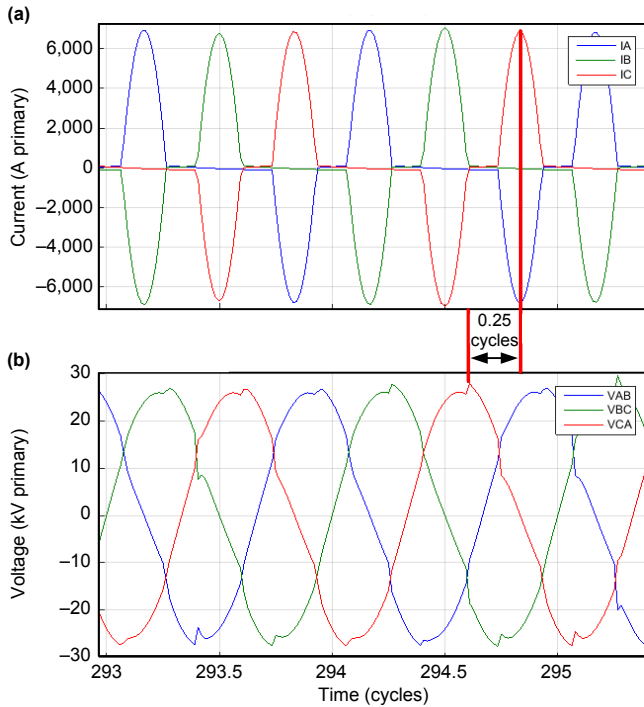


Fig. 24. Phase current (a) and phase voltage (b) relationship in simulation

Additional similarities can be seen between the event and simulated waveforms, as shown in Fig. 25.

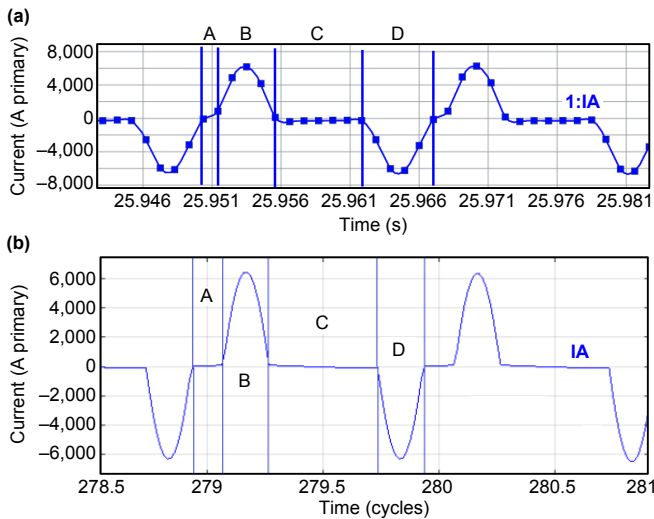


Fig. 25. Current waveform regions in the event data (a) and the simulation data (b)

The event and the simulation both have four regions in the current waveform. The high levels of current in Regions B and D indicate transformer core saturation. The lower levels of current in Regions A and C indicate no core saturation.

Analyzing the voltage waveforms reveals similar distortions in the event and simulation as well, as shown in Fig. 26.

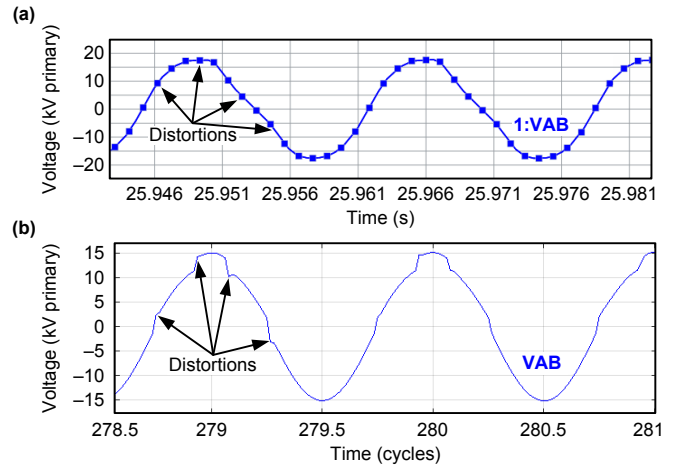


Fig. 26. Voltage waveform distortions in the event data (a) and the simulation data (b)

Once the transformer comes out of saturation, the currents and voltages regain their pure 60 Hz sinusoid nature and their magnitude is less than 100 A, similar to what was found in the event. Note that in our simulation the BH curve is piecewise and not as smooth as that of the real transformer. This allows us to illustrate the waveform distortions more clearly. This analysis led to the conclusion that the approximation of the system was acceptable based on the observed similarities between the simulation and event data during both transient and steady-state conditions.

The model also provided an explanation for the deviation of the third-harmonic element from its ideal ratio. The distortions in the voltage waveforms observed in Fig. 26 introduce a third-harmonic voltage at the neutral and the terminal of the generator, as shown in Fig. 27. Without transformer core saturation, there is no third-harmonic at the neutral and the terminal, as is expected from a source that generates purely fundamental voltages.

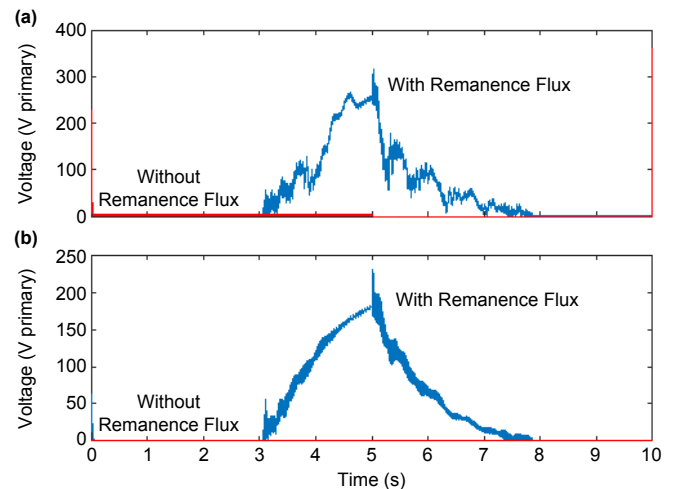


Fig. 27. Equivalent circuit during operation of the third-harmonic element for terminal third-harmonic voltage (a) and neutral third-harmonic voltage (b)

This phenomenon is discussed in [9] and can be represented by the circuit shown in Fig. 28. The external voltage source  $V_{3X}$ , introduced by the nonlinearity of the GSU, changed the third-harmonic circuit because of the presence of the interwinding capacitance [9], causing a deviation of the third-harmonic element from its ideal ratio. The root cause of this extreme nonlinearity was the residual flux left in the GSU transformer following the dc winding resistance testing. This residual flux in the transformer caused it to saturate as the generator field was applied, which caused the element to deviate from its well-defined profile and pickup.

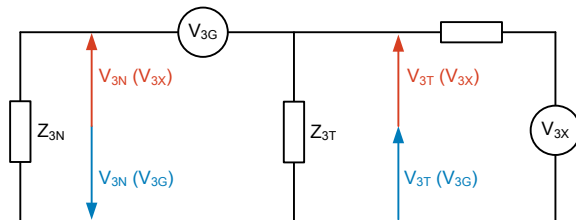


Fig. 28. Equivalent circuit during operation of the third-harmonic element

The values shown in Fig. 28 are defined as follows:

- $V_{3G}$  is the generator third-harmonic voltage.
- $Z_{3N}$  is the equivalent neutral impedance.
- $Z_{3T}$  is the generator terminal shunt impedance.
- $V_{3X}$  is the third-harmonic voltage caused by core saturation.
- $V_{3N}$  is the measured neutral voltage.
- $V_{3T}$  is the measured terminal voltage.

### B. Inadvertent Energization Element

The installed relay used the logic and timer settings in Fig. 12 for inadvertent energization protection. The field breaker status was brought into the relay using a normally closed auxiliary contact wired to IN102. The undervoltage element was set to 50 percent of nominal and the overcurrent element was set to 0.25 A secondary to ensure that the relay would detect an inadvertent energization through the auxiliary transformer.

Fig. 29 shows the current and voltage magnitudes as the field is applied. It also shows the status of the digital elements related to this element.

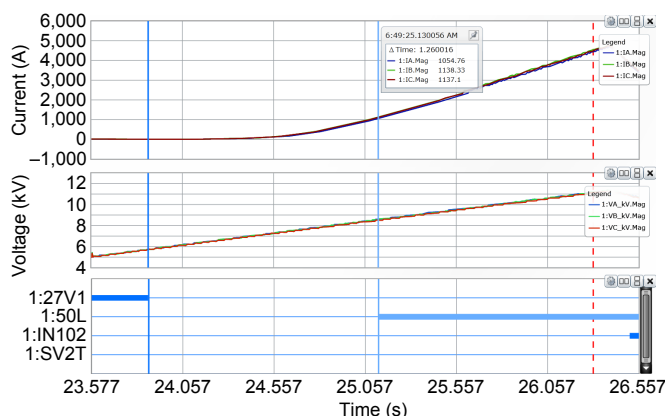


Fig. 29. Inadvertent energization event data

The field breaker status is deasserted throughout the event until the trip occurs. This confirms that the field breaker was closed prior to the beginning of the data capture.

The output of the arming/disarming timer is represented by the SV2T bit. Because this was already zero at the beginning of the event report data, it can be concluded that the field breaker had closed at least 1 second prior to the data capture. Therefore, because the logic was disarmed well before the appearance of inrush current, this logic was secure for this abnormal condition.

However, if the logic in Fig. 11 had been used instead, the dropout would have begun timing when the 27V1 element deasserted. Note that the overcurrent element (50L) asserted 1.26 seconds after 27V1 deasserted. This only left a margin of 0.26 seconds. Had the voltage been set to ramp faster, the undervoltage element been set higher, or the dropout timer been extended, the logic in Fig. 11 could have operated for this case. Therefore, these event data confirm that the logic in Fig. 12 provides better security than the scheme in Fig. 11.

### C. Phase Differential Element

Based on the discussion in Section III, Subsection C, spurious differential current was not expected during this event because the GSU transformer consisted of three single-phase transformers. Fig. 30 shows the operate and restraint values for each phase of the generator differential protection.

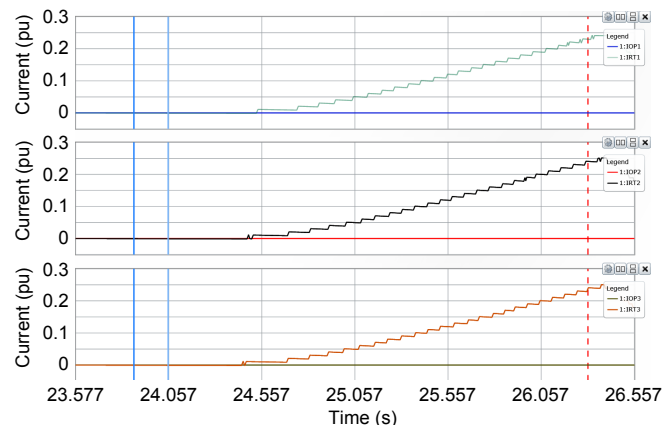


Fig. 30. Phase differential event data for three single-phase GSU transformers

Fig. 30 confirms that no differential current was seen by the relay. It also shows that the peak current was approximately 0.25 pu.

Another generator at this facility with a single three-phase GSU transformer was later returned to service following dc winding resistance testing. These data are shown in Fig. 31. In this case, the current magnitudes varied on each phase, but none of them exceeded 0.2 pu. As such, the CTs were not driven to saturation. However, the CTs used on this unit were quite large, so it should not be assumed that CT saturation and differential current cannot occur for this type of transformer, for the reasons discussed in Section III, Subsection C.

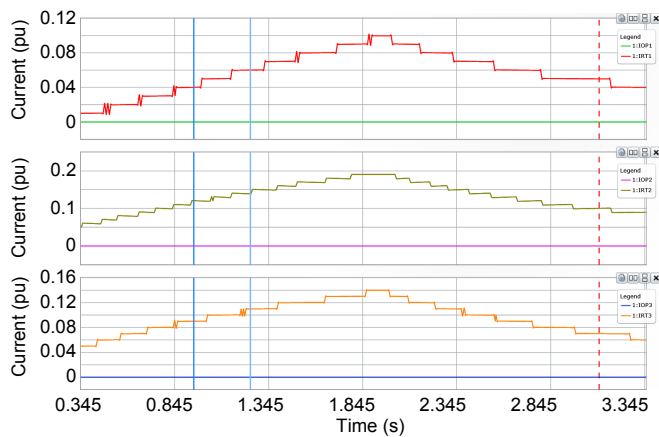


Fig. 31. Phase differential event data for a three-phase GUS transformer

## V. SOLUTIONS TO IMPROVE THE SECURITY OF THE THIRD-HARMONIC ELEMENT

This section discusses various methods that can be implemented to improve the security of the third-harmonic differential element and avoid a misoperation.

### A. Demagnetize the GUS Transformer Following Testing

The best method to address this issue is to remove the source of the inrush current by demagnetizing the GUS transformer following dc winding resistance testing. Adding this step to the testing procedure limits the inrush to normal levels when the field is applied, thus preventing the distortion of the third-harmonic profile and the larger currents that can threaten the security of the protection elements. Refer to [6] for a discussion of methods to demagnetize a transformer core.

However, transformer dc winding resistance testing might be done only once every 7 to 8 years, depending on the maintenance program. It may not be desirable to modify the procedure for a test done so infrequently. In this case, there are some options that can be included in the protection scheme to add security, as discussed in the following subsections.

### B. Increase Pickup of the Third-Harmonic Differential Element

During commissioning of the third-harmonic differential element using generator load data, a ratio of 0.8 was observed between the third-harmonic secondary neutral voltage ( $V_{3N}$ ) and the third-harmonic secondary terminal voltage ( $V_{3P}$ ). To ensure a proper overlap in the stator winding coverage of at least 10 percent between the neutral fundamental overvoltage element and the third-harmonic differential element, a pickup of 0.5 was chosen. Fig. 32 shows the winding coverage of both 64G1 (59N) and 64G2 (59THD) with the lower-winding side overlap being 15.6 percent.

Fig. 33 shows how increasing the pickup setting of the third-harmonic differential element improves the security during a GUS inrush condition. However, increasing the pickup setting reduces the element sensitivity and is not necessarily desirable. In this case, changing the 64G2 element pickup from 0.5 to 1.3 also reduces the overlap between the 64G1 and 64G2 elements from 15.6 percent to 2.9 percent.

This is not an acceptable level of margin. A minimum overlap of 10 percent is usually recommended.

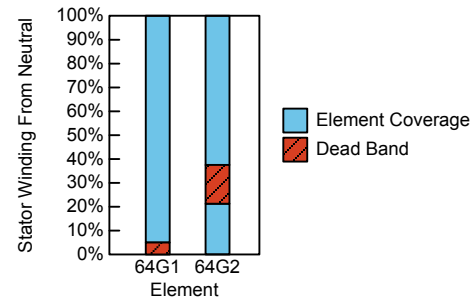


Fig. 32. Winding coverage of ground fault protection elements based on commissioning data

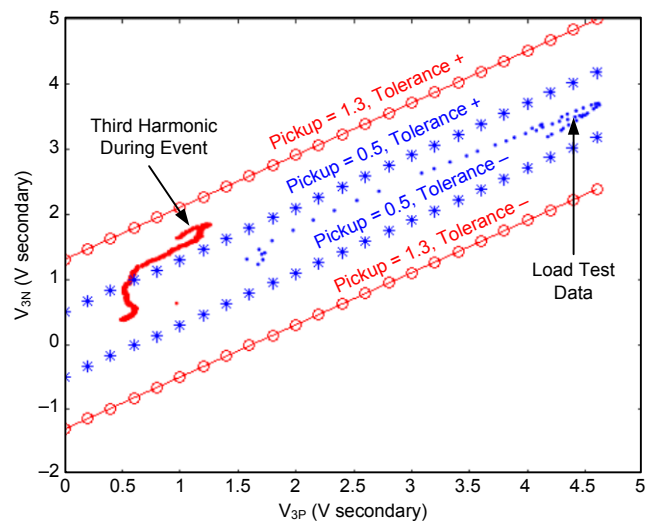


Fig. 33. Third-harmonic profile of machine with third-harmonic differential element characteristic

Although this is not an acceptable solution for continuous operation, it may be possible to apply this concept to temporary settings. The increased pickup setting is only required to provide security while the field is ramping. Note that the generator is offline and not connected to the grid at this time, hence the pickup setting of 64G2 (59THD) can be increased. This provides security during the field ramp while providing the necessary sensitivity for normal operation.

A typical method to modify the pickup setting in modern digital relays is to change setting groups. However, changing setting groups can disable protection in a relay for up to a few seconds, and the impact of this loss of protection should be evaluated.

### C. Use More Secure Supervisory Checks

#### 1) Time-Delayed Voltage Supervision

The third-harmonic differential element for this generator was enabled once the positive-sequence terminal voltage exceeded 50 percent of the rated voltage. To add more security to the element, the element could be delayed because inrush conditions do disappear eventually. The delay setting might be difficult to set because an inrush condition when a transformer is energized with a step voltage change does not

last as long as one that has a field ramp applied to it. This increases the complexity of the delay setting.

However, the third-harmonic differential element is a sensitive element that is designed to provide ground fault protection to the bottom 5 percent of the windings near the neutral of the generator. There are two main concerns for faults in this region. If a ground fault occurs in the bottom 5 percent of the winding as a result of a breakdown of the ground insulation, the fault current is very small and the damage is typically assumed to be minimal. However, if a second fault occurs in the generator, this fault current will not be limited because the grounding transformer has effectively been bypassed by the first fault.

The second concern is for a ground fault that occurs as the result of a break in the load-carrying conductor. In this case, the fault will cause arcing as current continues to flow and the resulting damage can be substantial if ground fault protection is not provided for this region. Therefore, there is some risk associated with adding an arming delay that must be evaluated. In order to gain security, it may be considered acceptable to assume this risk, but it is recommended that the arming delay be kept to a minimum to ensure the fast detection and isolation of ground faults that occur while applying the field.

In the case study covered in this paper, this is the solution that was implemented.

#### 2) Sync-Breaker Status Supervision

Another supervision option is the usage of the sync-breaker status to enable the element once the generator is online. For the generator where the event occurred, there was a 5-minute window between when the field was applied and when the sync breaker was closed. This delay is more than enough to ensure that the inrush condition has subsided before enabling the element.

One possible issue with this scheme is that a ground fault cannot be detected until the unit is already synchronized to the grid. This is not desirable in many cases.

#### D. Temporarily Block Protection Following Testing

As mentioned previously, dc winding resistance testing is not performed frequently. Therefore, another method to avoid an unintended operation is to manually block the third-harmonic element after dc resistance testing. After allowing sufficient time for the inrush to subside, the protection can be reenabled. However this method provides security by means of lack of availability and may not be desirable.

In addition, a human factor is also involved, and there is a possibility that the protection might not be blocked, potentially leading to an undesired operation. The opposite is also true in that the protection could remain disabled indefinitely, making the protection system blind to faults in the bottom 5 percent of the winding.

#### E. Use Additional Relay Logic to Limit Coverage to the Neutral

The generator relay used in the case study provides digital bits that indicate whether the fault occurred in the upper (T64G) or the lower portion (N64G) of the stator windings, as shown in Fig. 34.

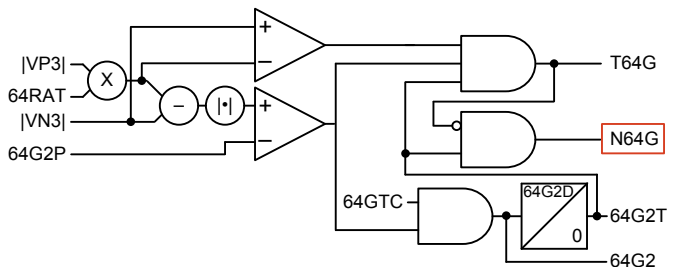


Fig. 34. Ground fault protection elements of a generator relay

Because the neutral overvoltage function provides reliable ground-fault protection for the upper set of stator coils, the third-harmonic differential element can be used to provide sensitive protection for only the lower portion of the stator winding while improving the security of the scheme.

It should be noted that although this change significantly improves the element security and would have made the element secure for the event discussed in this paper, it does not guarantee security for all cases. It is possible that the transformer third-harmonic source could have the opposite effect on the neutral-to-terminal third-harmonic voltage ratio, as in the case of a GSU transformer with a DAB winding.

#### F. Use the Subharmonic Injection Method

Subharmonic injection is an alternative method that can provide 100 percent stator ground fault protection. Using a subharmonic injection source at the neutral of the machine allows for an impedance measurement at the injected frequencies to detect a ground fault in the generator. Because transformer inrush does not exhibit these subharmonic frequencies, this method provides a very secure yet sensitive operating principle while being easy to set. Because of these benefits, this method has been increasingly popular in recent years.

## VI. CONCLUSION

This paper discusses transformer dc winding resistance testing, with specific attention given to the residual flux that is often left in the transformer. The expected inrush current waveforms upon re-energization of a transformer containing residual flux are described in detail.

Based on the expected currents and voltages, three generator protection elements that could be affected are discussed, and their respective performance under these abnormal conditions are analyzed.

A case study is presented involving the operation of a third-harmonic voltage differential element when the field was applied following dc winding resistance testing. The event report data are analyzed and compared to a system model. The simulation data clearly resembled the event report data captured by the relay. The verified model provided insight into the behavior seen in the event and the root cause of the third-harmonic element operation.

Based on the event analysis, several possible solutions for improving the scheme security are provided. The benefits and shortfalls of each option are presented. The optimum solution may vary from one application to another and may also be a combination of two or more of the solutions presented.

## VII. ACKNOWLEDGMENT

The authors would like to thank the engineers and technicians who willingly shared the data for this case study. They would also like to thank Rogerio Scharlach, Jim Buff, Normann Fischer, and Dale Finney for their assistance in analyzing this event.

## VIII. REFERENCES

- [1] U.S. Department of Energy, Office of Electricity Delivery and Energy Reliability, "Large Power Transformers and the U.S. Electric Grid," June 2012. Available: <http://energy.gov>.
- [2] S. Hodder, B. Kasztenny, N. Fischer, and Y. Xia, "Low Second-Harmonic Content in Transformer Inrush Currents – Analysis and Practical Solutions for Protection Security," proceedings of the 67th Annual Conference for Protective Relay Engineers, College Station, TX, March 2014.
- [3] IEEE Standard C57.152-2013, IEEE Guide for Diagnostic Field Testing of Fluid-Filled Power Transformers, Regulators, and Reactors.
- [4] EPRI, *Power Transformer Maintenance and Application Guide*. Electric Power Research Institute, Inc., Palo Alto, CA, September 2002.
- [5] B. Hembroff, M. Ohlen, and P. Werelius, "A Guide to Transformer Winding Resistance Measurements," April 2009. Available: <http://www.avo.co.nz/>.
- [6] M. Pütter, M. Rädler, and B. Unterer, "Reliable Demagnetization of Transformer Cores," July 2014. Available: <https://www.omicronenergy.com>.
- [7] IEEE Power System Relaying Committee (PSRC), *IEEE Tutorial on the Protection of Synchronous Generators*. Second edition, 2011. Available: <http://www.pes-psrc.org>.
- [8] M. Donolo, A. Guzmán, M. V. Mynam, R. Jain, and D. Finney, "Generator Protection Overcomes Current Transformer Limitations," proceedings of the 41st Annual Western Protective Relay Conference, Spokane, WA, October 2014.
- [9] N. Klingerman, D. Finney, S. Samineni, N. Fischer, and D. Haas, "Understanding Generator Stator Ground Faults and Their Protection Schemes," proceedings of the 42nd Annual Western Protective Relay Conference, Spokane, WA, October 2015.

## IX. BIOGRAPHIES

**Ritwik Chowdhury** received his bachelor of engineering degree from the University of British Columbia and is currently pursuing a master of engineering degree at the University of Toronto. He joined Schweitzer Engineering Laboratories, Inc. in 2012 as a power engineer in R&D and now serves as an application specialist. His research interests include the analysis and control of generators and their systems, power converters, and generator and line protection. He is a member of IEEE.

**Mircea Rusciur** graduated from the University of Waterloo in 2012 with a B.A.Sc. in electrical engineering and an option in management sciences. He joined Schweitzer Engineering Laboratories, Inc. in 2012 as an application engineer in Barrie, Ontario, Canada, and he is a registered professional engineer in the province of Ontario.

**Jason Young** graduated from the University of Waterloo in 2006 with a B.A.Sc. in electrical engineering. He joined Schweitzer Engineering Laboratories, Inc. in 2006, where he currently serves as an application engineer in Smiths Falls, Ontario, Canada. He is a registered professional engineer in the province of Ontario and an IEEE member.

**Jakov Vico** graduated from the University of Belgrade, Serbia, in 1986 with a B.Sc. and an M.Sc. in electrical power engineering. He joined Schweitzer Engineering Laboratories, Inc. as a senior application engineer in 2012. Presently, he is the Toronto branch manager with 28 years of utility and industrial electrical system protection experience. He is a registered professional engineer in Ontario, Manitoba, Prince Edward Island, Newfoundland and Labrador, New Brunswick, and Nova Scotia. He is a senior IEEE member.